International Journal of Heat and Fluid Flow 29 (2008) 1512–1526

Contents lists available at ScienceDirect

International Journal of Heat and Fluid Flow

journal homepage: www.elsevier.com/locate/ijhff

Experimental hot-wire measurements in a centrifugal compressor with vaned diffuser

Ali Pinarbasi *

Department of Mechanical Engineering, Engineering Faculty, Cumhuriyet University, 58140, Sivas, Turkey

ARTICLE INFO

Article history:
Received 5 March 2008
Received in revised form 15 April 2008
Accepted 23 April 2008
Available online 12 June 2008

Keywords:
Diffuser flow
Vaned diffuser
Compressor

ABSTRACT

The purpose of this study was to improve the understanding of the flow physics in a centrifugal compressor with vaned diffuser. For this reason three component hot wire measurements in the vaneless space and vane region of a low speed centrifugal compressor are presented. A low speed compressor with a 19 bladed backswept impeller and diffuser with 16 wedge vanes were used. The measurements were made at three inter-vane positions and are presented as mean velocity, turbulent kinetic energy and flow angle distributions.

The flow entering the diffuser closely resembles the classic jet-wake flow characteristic of centrifugal impeller discharges. A strong upstream influence of the diffuser vanes is observed which results in significant variations in flow quantities between the vane-to-vane locations. The circumferential variations due to the passage and blade wakes rapidly mix out in the vaneless space, although some variations are still discernible in the vaned region. The impeller blade wakes mix out rapidly within the vaneless space and more rapidly than in an equivalent vaneless diffuser. Although the flow is highly non uniform in velocity at the impeller exit, there is no evidence in the results of any separation from the diffuser vanes.

1. Introduction

Vaned diffusers are applied in a wide variety of compressor applications. Their impact on the operating range of a single stage compressor depends upon such parameters as impeller performance, number of vanes, vaneless space ratio, vane thickness and leading edge configuration.

The vaneless space ratio is very sensitive in the diffuser design as it is related with throat blockage. When the location of the vane leading edge is close to the impeller it is known that, there is increased noise level, increased vibration and high Mach numbers result at the vane leading edge.

Yoshinaga (1980) used 16 different vaned diffusers for an experimental investigation to improve the stage efficiency. In their results, the vaned diffuser showed about 4% higher efficiency than the vaneless diffuser for the same diffuser outlet radius.

Another experimental study using vaneless and vaned diffusers was conducted by Inoue and Cumpsty (1984). They observed that, the circumferentially averaged mean radial velocity profile in the axial direction for the vaned diffuser inlet was almost identical with that for the vaneless diffuser. In the low radial velocity region near the diffuser vane leading edge reversed flow was observed at low flow rates and this led to an increase of loss near the side walls. Strong reversed flow appeared near the diffuser vane leading edge, near the shroud and the hub when the flow rate was decreased.

An investigation of impeller and diffuser flow was undertaken by Krain (1981), in a flat straight channel diffuser with a splitter blade impeller. The flow in the vaned diffuser entrance region was highly distorted and of an unsteady nature.

These studies indicate that flow is highly distorted near the leading edge of the vane, but a well designed vaned diffuser may moderate these non-uniformities within the vanes. The purpose of the current experimental investigation was to measure the detailed flow in a vaned diffuser. The vanes are fitted within a similar vaneless diffuser to that used in previous studies by Pinarbasi and Johnson (1994, 1995, 1996).

2. Experimental details

The experimental work was carried out using the low speed centrifugal compressor test rig shown in Fig. 1. The original impeller geometry is given by Johnson and Moore (1980), but for the current study the radial outlet section was replaced to give a 30° backswept outlet angle as detailed by Farge and Johnson (1990). The shrouded impeller had 19 blades and was one meter in diameter. The vaned diffuser (Fig. 2) contained 16 wedge type blades which were mounted at an angle of 45° in order to give zero incidence angle at the leading edge. Table 1 shows the principal specifications of the vaned diffuser. The vaneless space ratio of 1.1 was

* Tel.: +90 346 2191339; fax: +90 346 219 11 75.
E-mail address: alipinarbasi@cumhuriyet.edu.tr

0142-727X/$ - see front matter © 2008 Elsevier Inc. All rights reserved.
doi:10.1016/j.ijheatfluidflow.2008.04.011

Nomenclature

A, B, c	King's law calibration coefficients
E	hot wire anemometer voltage
h, k	directional coefficients for hot wire
L	radial distance from impeller outlet
q	non-dimensional turbulent kinetic energy
R_o	impeller outlet radius
R	radial coordinate
U_e	effective cooling velocity
U_T	peripheral blade velocity at the impeller outlet
U_n, U_t, U_b	normal, tangential and binormal velocity components relative to the wire
u_θ, u_r, u_z	tangential, radial and axial mean velocity components
u'_θ, u'_r, u'_z	tangential, radial and axial r.m.s fluctuating velocity components
y/y_o	circumferential coordinate
z/z_o	axial coordinate

selected as a typical value (for example Inoue and Cumpsty, 1984; Krain, 1981; Hayami, 1990).

The vane design gives a constant cross-sectional flow area through the vaned part of the diffuser and hence the absolute Mach number of 0.1 is constant throughout. This design was chosen so that comparisons could be made with the previous work carried out in a constant cross-sectional flow area vaneless diffuser.

2.1. Measurement method

The measurements were made using hot wire anemometry. Three mutually perpendicular wires were used with a single wire Dantec (55P11) oriented in the circumferential direction and a double wire probe Dantec (55P61) oriented in the axial radial plane. A shaft encoder is used to control the simultaneous sampling of the output voltages from the three hot wire anemometers. The three hot wire anemometer voltages are first converted to the three corresponding effective wire cooling velocities using King's law. According to King's Law for each wire, the voltage E is related to the effective cooling velocity U_e by the following relationships

$$E^2 = A + BU_e^c \tag{1}$$

where A represents the heat loss through natural convection and conduction along the prongs at zero velocity. The coefficients A, B and c are determined by calibration of each wire in a wind tunnel.

Directional sensitivity of the wires was undertaken to determine the relationship between the effective wire cooling velocities and mutually perpendicular velocity components. Each of the instantaneous velocity components, according to Jorgensen (1971),

$$\begin{aligned} U_{1e}^2 &= k^2U_n^2 + U_t^2 + h^2U_b^2 \\ U_{2e}^2 &= h^2U_n^2 + k^2U_t^2 + U_b^2 \\ U_{3e}^2 &= U_n^2 + k^2U_t^2 + h^2U_b^2 \end{aligned} \tag{2}$$

where U_n, U_t and U_b are the normal, tangential and binormal velocity components relative to the wire. Coefficients h and k were determined by changing the wire orientation at fixed wind tunnel speed. The probe was rotated through a range of ±50° yaw and 20° pitch angles. The errors in the measured velocity and flow direction resulting from this procedure were estimated to be ±1 m/s and ±5°, respectively. The majority of this error results from the assumption of constant coefficients in Eq. (1) and particularly in Eq. (2). Discrepancies thus result between the calibration values and the fitted calibration equations, particularly for large flow angles. Following calibration, measurements were made at 14 axial measurement locations on each passage cross section for different diffuser locations and flow rates. At each position readings were performed on each of 230 shaft revolutions at 1/3° interval of shaft rotation spanning one impeller passage. The mesh of data points is thus $8 \times 14 \times 57$ in the radial, axial and tangential directions, respectively. In the case of the vaned diffuser, measurements were repeated at three diffuser vane to vane positions (10%, 50% and 90%).

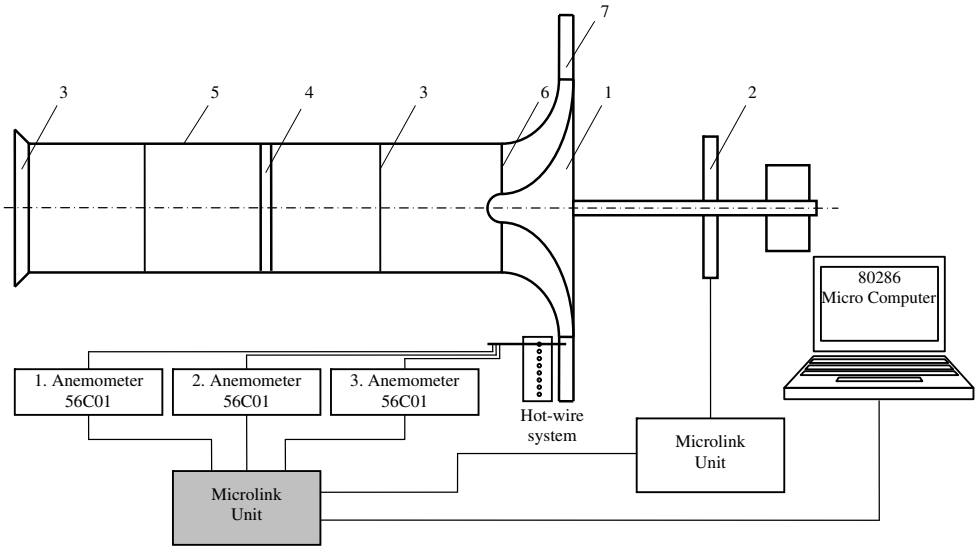

1-Impeller 2-Pulley Driven by motor 3-Screens 4-Honeycomp 5-Inlet Duct 6-Seal 7-Diffuser

Fig. 1. Schematic of centrifugal compressor test rig.

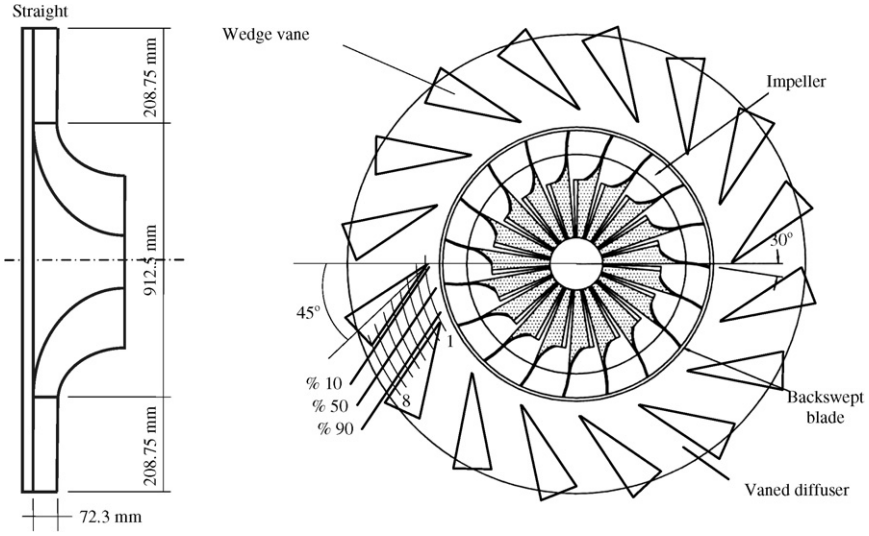

Fig. 2. Diffuser details.

Table 1
Geometry, operating condition and measurement locations

Impeller								
Inlet blade radius at the hub					$R_h = 88.75$ mm			
Inlet blade radius at the shroud					$R_s = 283.75$ mm			
Outlet radius					$R_o = 454.6$ mm			
Backswept blade angle					$\beta = 30°$			
Number of the blades					$N = 19$			
Outlet blade span					$b = 72.3$ mm			
Rotating speed					$n = 500$ rpm			
Mass Flow rate					$m = 0.1311$ kg/s			
Mean absolute outlet flow angle					$\alpha = 45°$			
Vaned diffuser								
Vane geometry					Wedge (included angle 22.5°)			
Vane angle					45°			
Number of vanes					16			
Inlet/outlet area ratio					1			
Diffuser throat width					178.5 mm			
Diffuser inlet diameter					912.5 mm			
Diffuser outlet diameter					1524 mm			
Channel length					208.75 mm			
Vane span					72.3 mm			
Vaneless space radius ratio					1.1			
Length/width ratio					0.37			
Measurement locations								
Station	1	2	3	4	5	6	7	8
L/R_o	0.02	0.08	0.15	0.21	0.27	0.33	0.39	0.45

3. Analysis of results

Mean velocity and normal stress components are calculated statistically considering 230 consecutive impeller revolutions at each measurement point. Mathematically mean velocity and Reynolds stress components are determined through Eqs. (3) and (4), respectively. Eq. (1) is firstly used to convert instantaneous voltage reading to an instantaneous effective cooling velocity for each wire. Eq. (2) is then used to determine the three mutually perpendicular instantaneous velocity components.

$$\bar{u}_i = \frac{1}{230}\sum_{m=1}^{230} u_i \quad i = r, \theta, z \tag{3}$$

$$\overline{u_i'^2} = \frac{1}{230}\sum_{m=1}^{230}(u_i - \bar{u}_i)^2 \quad i = r, \theta, z \tag{4}$$

The turbulent kinetic energy is defined as

$$q = \frac{1}{230}\sum_{m=1}^{230}\frac{\overline{u_r'^2 + u_\theta'^2 + u_z'^2}}{2U_T} \tag{5}$$

where U_T is the blade velocity at the impeller outlet.

An error analysis indicated that the uncertainties in the mean velocity components and turbulent kinetic energy components were ±1 m/s, ±0.1% and ±0.05%, respectively. The majority of this error results from the assumption of constant coefficients in Eq. (1) and particularly Eq. (2). Discrepancies thus results between the calibration values and fitted calibration equations particular large flow angles.

4. Experimental results

In this paper, results at four critical stations (Station 1, 2, 3 and 8) are considered. Station 1 is located in the diffuser vaneless space, Station 2, just entry region but Station 3 is located in the vaned part of the diffuser and Station 8 is located at the exit section of the diffuser.

The mean velocities are presented as contour diagrams. The contours indicate the magnitude of the radial velocities and the secondary velocities are represented by arrows. The tangential margins of each diagram ($y/y_o = 0$ and 1) for each of the three vane to vane positions correspond to consecutive positions where the measurement probe is radially in line with the impeller blade trailing edge, thus each diagram shows how the flow varies at a particular diffuser vane to vane position and station as one impeller passage passes this position.

4.1. Station 1

Station 1 is located within the vaneless space close to impeller exit. The three inter vane position mean velocity results for station 1 are shown in Fig. 3. The results show *how, if* the flow rate is computed from the radial velocities, the flow rate adjacent to the vanes is reduced with a corresponding increase in the flow rate midway between the vanes. The peak level of radial velocity midway between the vanes is thus 3 m/s higher than close to the vanes. Strong cross flows are observed within the impeller passage wake in the pressure side shroud quarter. This is because the wake is increasing in size due to a decrease in velocity within it. The wake is less marked at the 90% vane-to-vane location which suggests that the pressure in this region may be lower at this location.

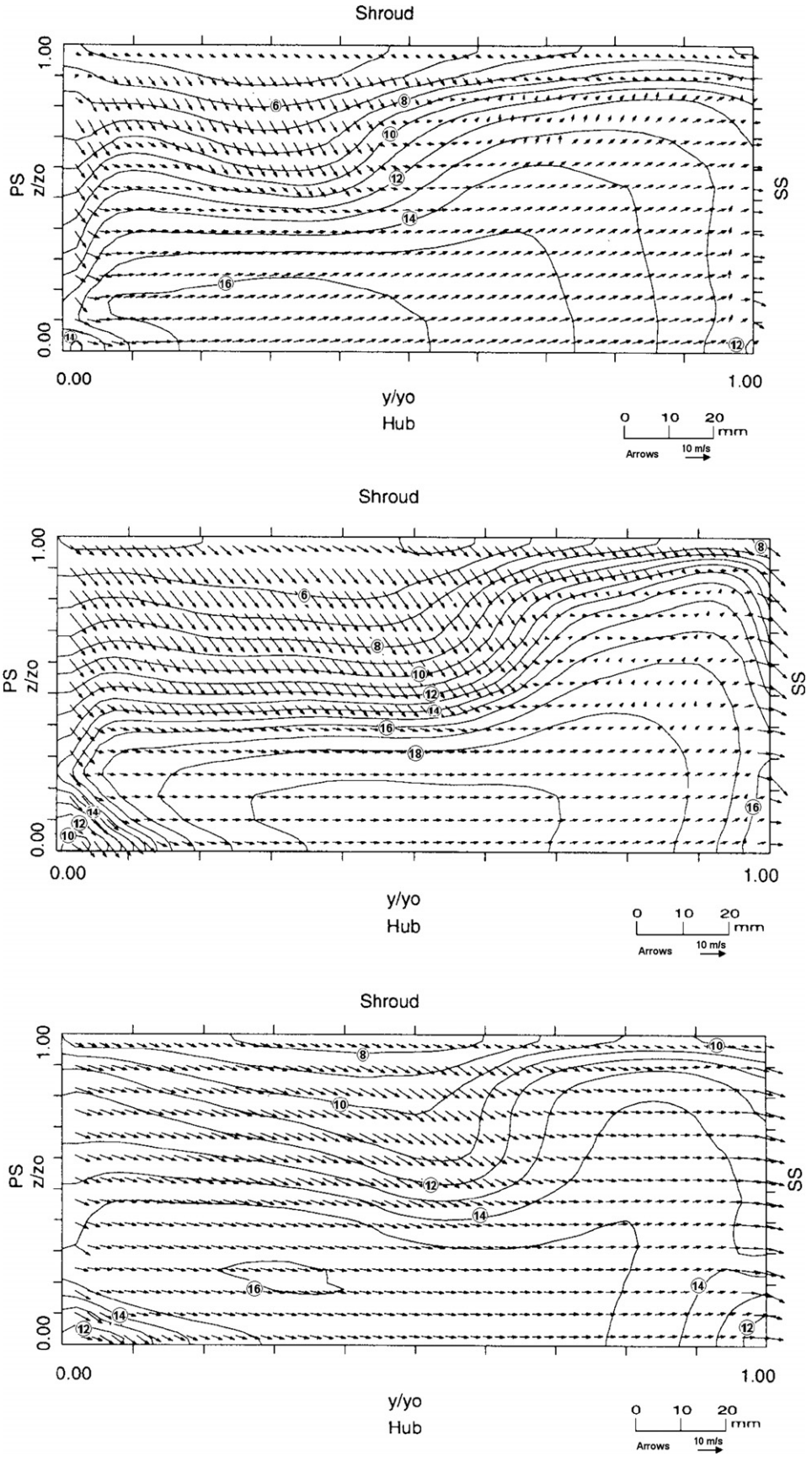

Fig. 3. Mean velocities at station 1 (10%, 50% and 90% vane-to-vane position).

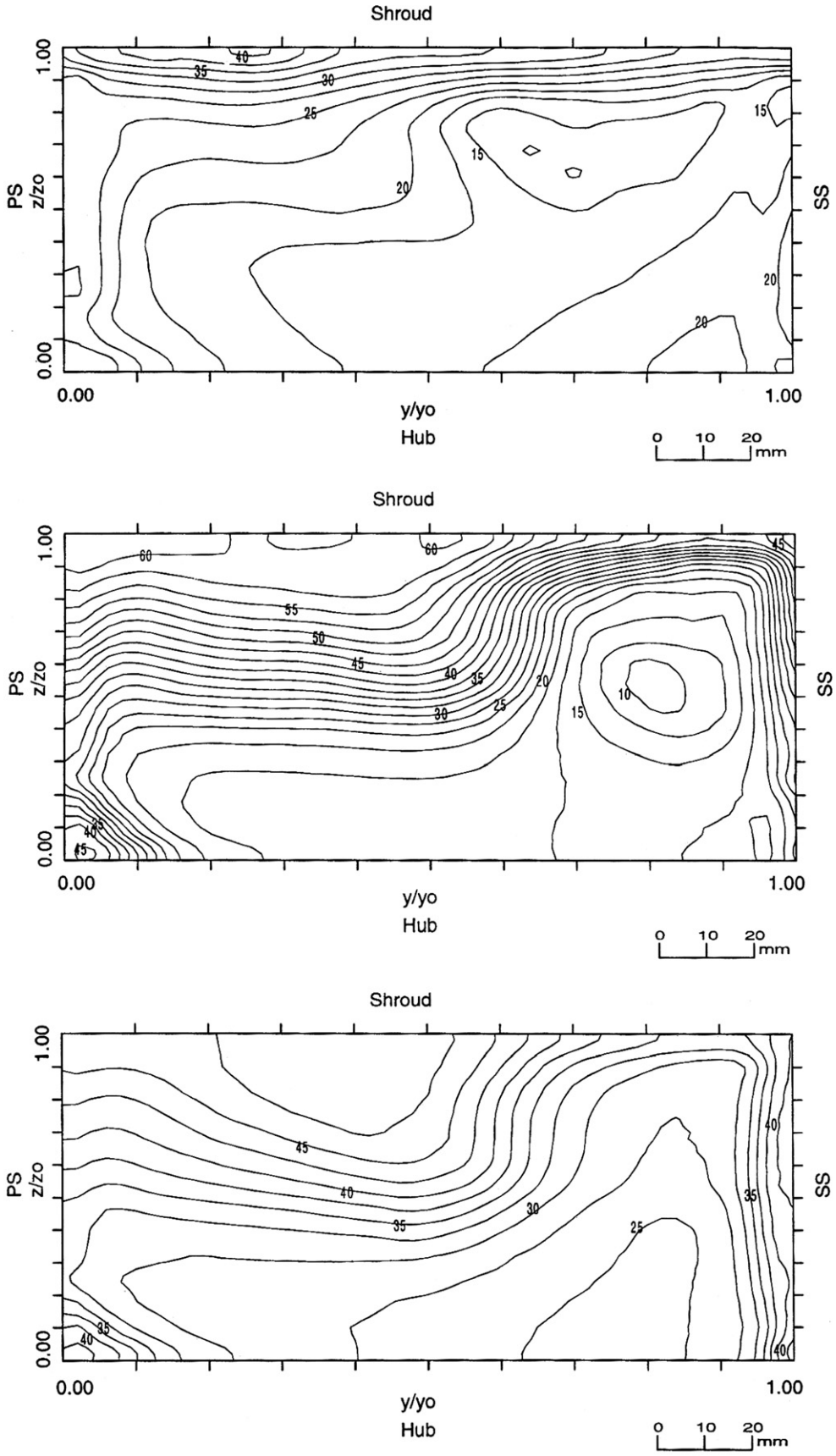

Fig. 4. Flow angle at station 1 (10%, 50% and 90% vane-to-vane position).

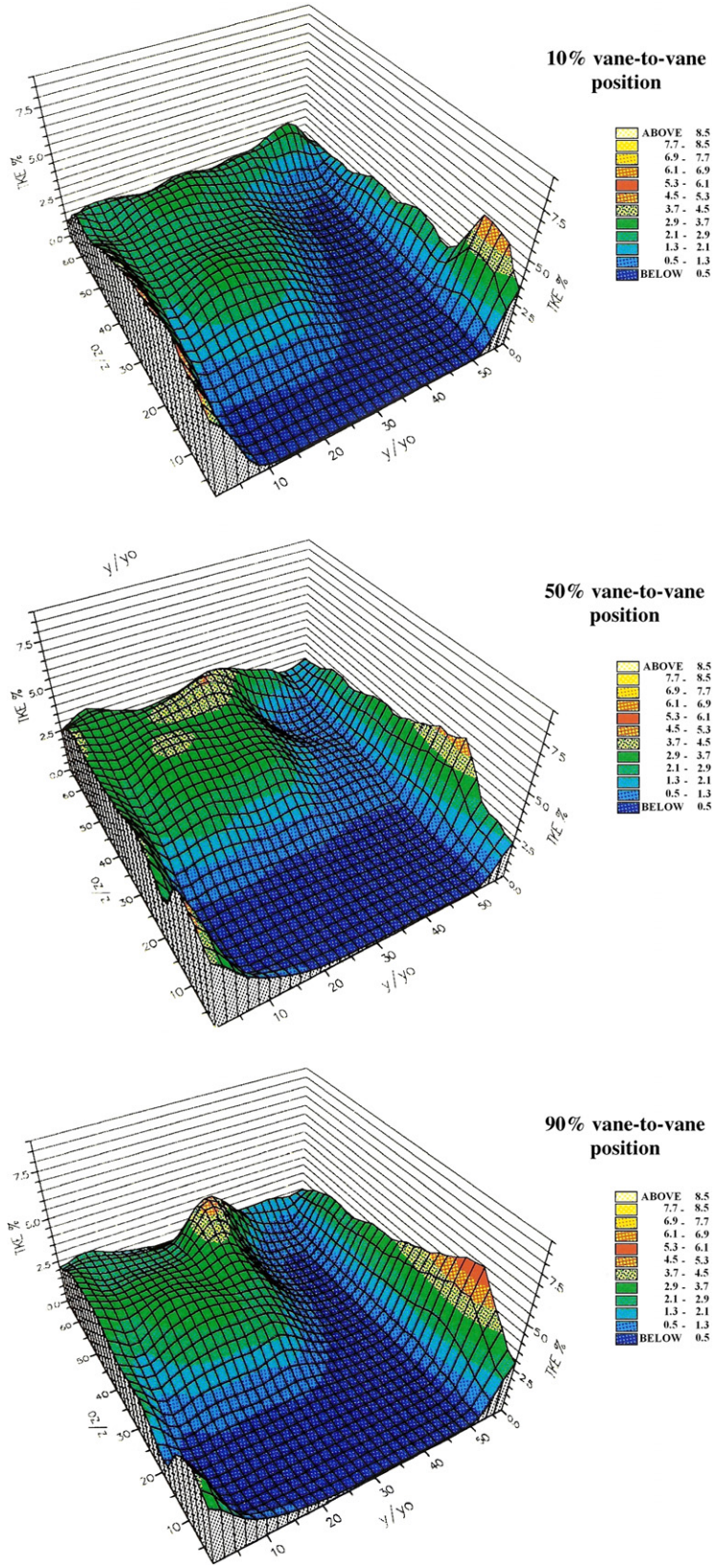

Fig. 5. Turbulent kinetic energy at station 1 (10%, 50% and 90% vane-to-vane position).

Fig. 4 shows that the vanes also moderate the circumferential variation in the absolute flow angle ($\tan^{-1}(u_\theta/u_r)$). The variation is generally less than 10° near the vanes, whereas 30° variations are observed at the mid vane position.

The turbulent kinetic energy distributions (Fig. 5) clearly show a substantial increase from less than 1% in the majority of the passage to between 6% and 8% within the blade wake. This level within the blade wake is however less than was observed for a

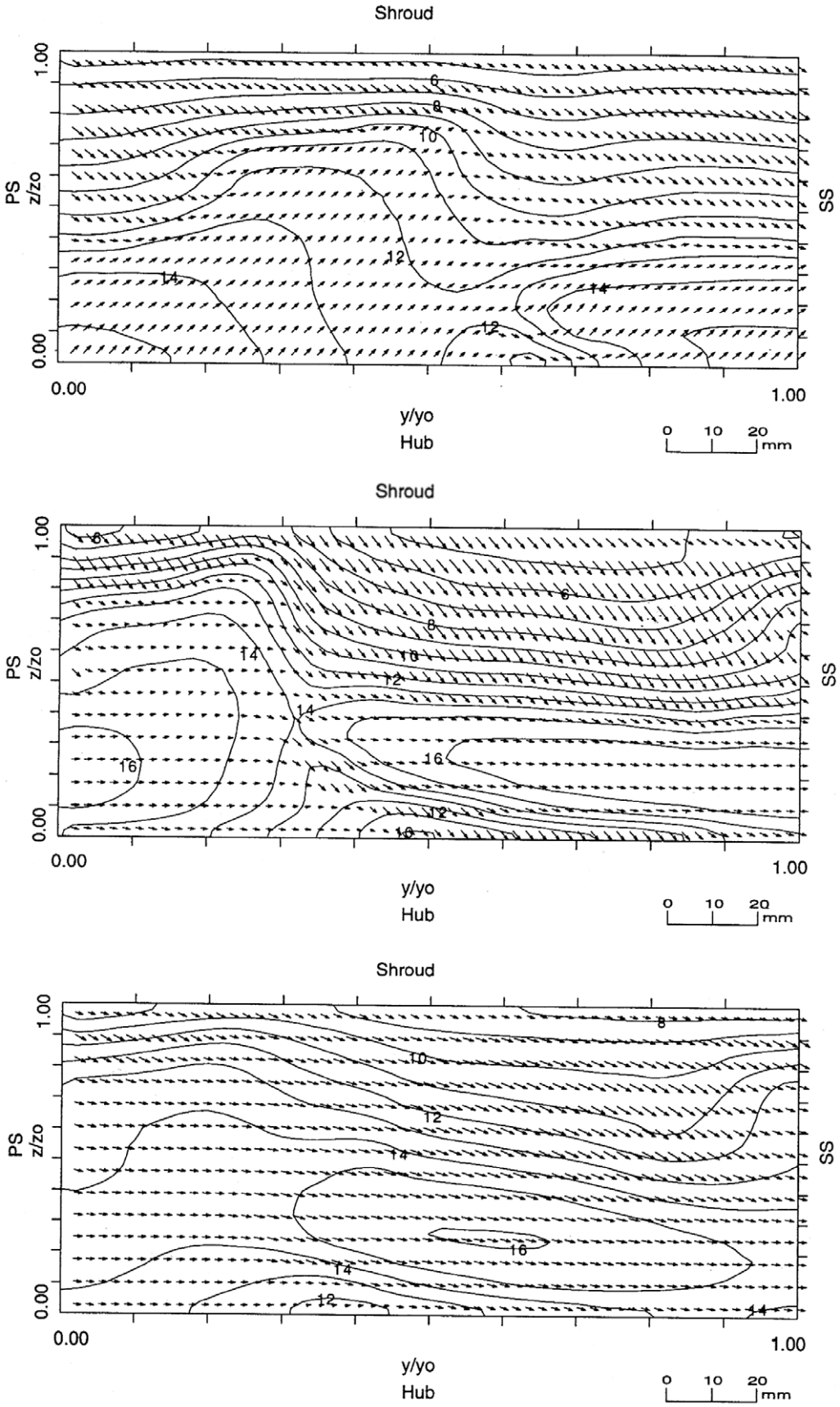

Fig. 6. Mean velocities at station 2 (10%, 50% and 90% vane-to-vane position).

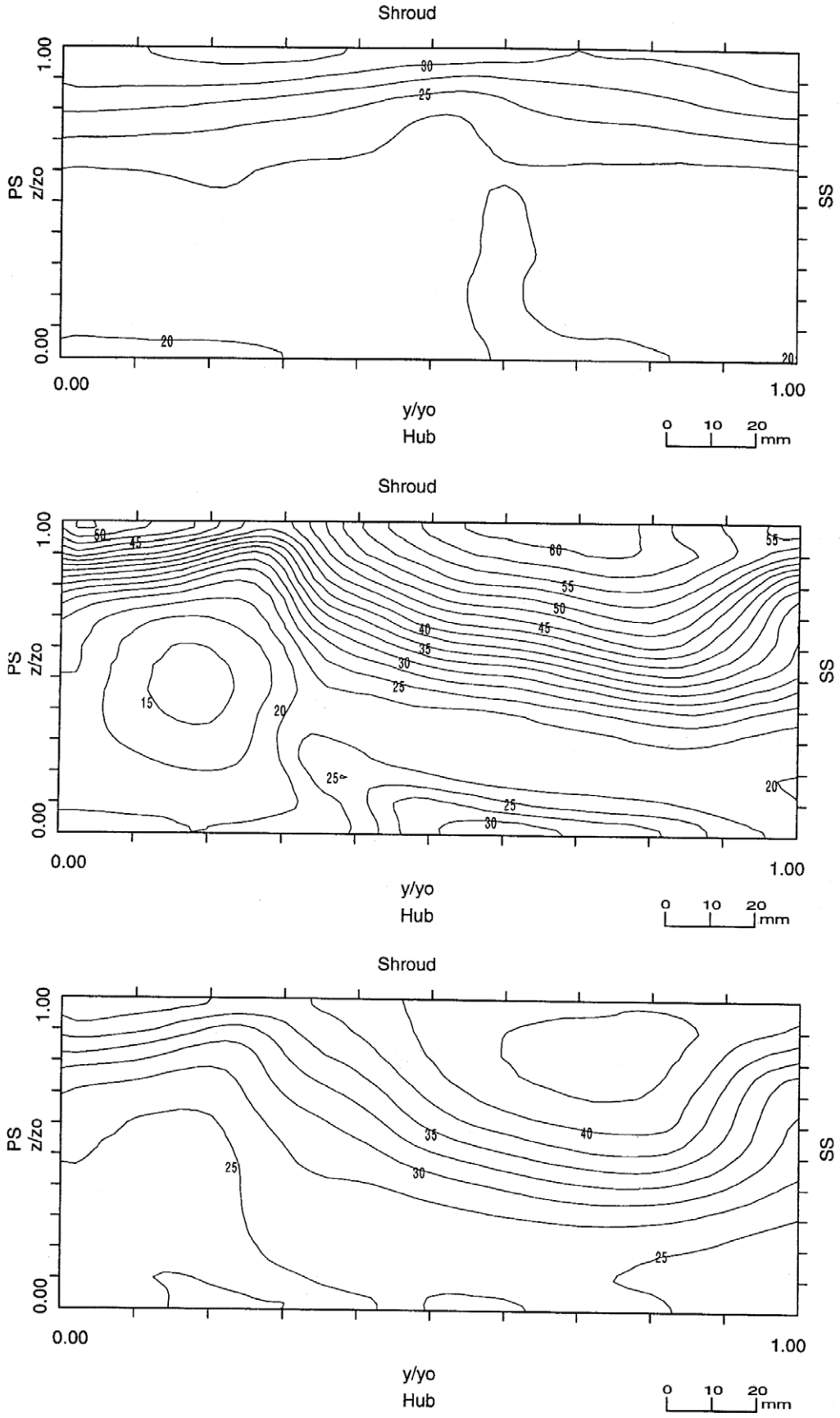

Fig. 7. Flow angle at station 2 (10%, 50% and 90% vane-to-vane position).

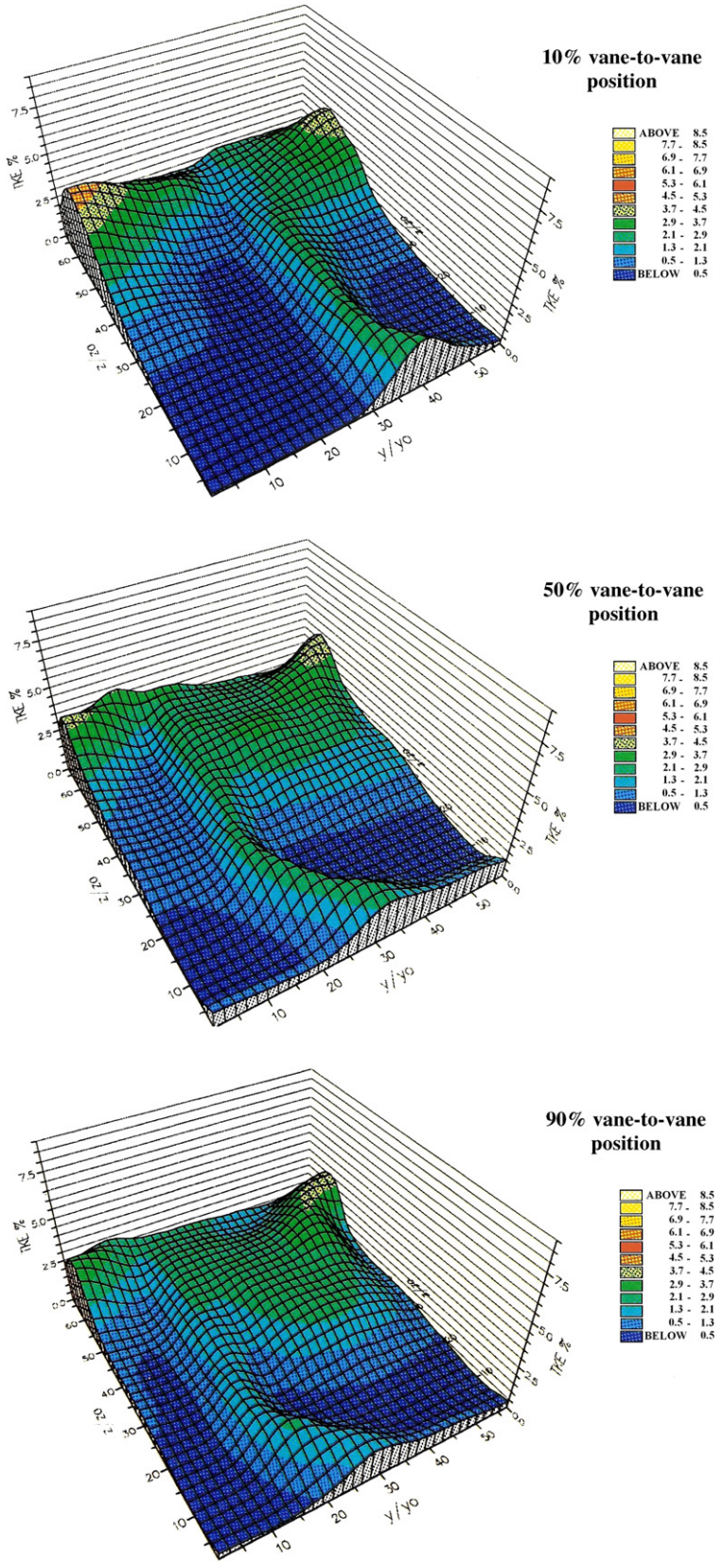

Fig. 8. Turbulent kinetic energy at station 2 (10%, 50% and 90% vane-to-vane position).

vaneless diffuser downstream of the same impeller (Pinarbasi and Johnson (1994)). This is because the blade wake is weaker in the vaned diffuser as it mixes out more rapidly downstream of the impeller blade. Enhancement of the mixing out is believed to be due to the periodic unsteadiness induced by the diffuser vanes.

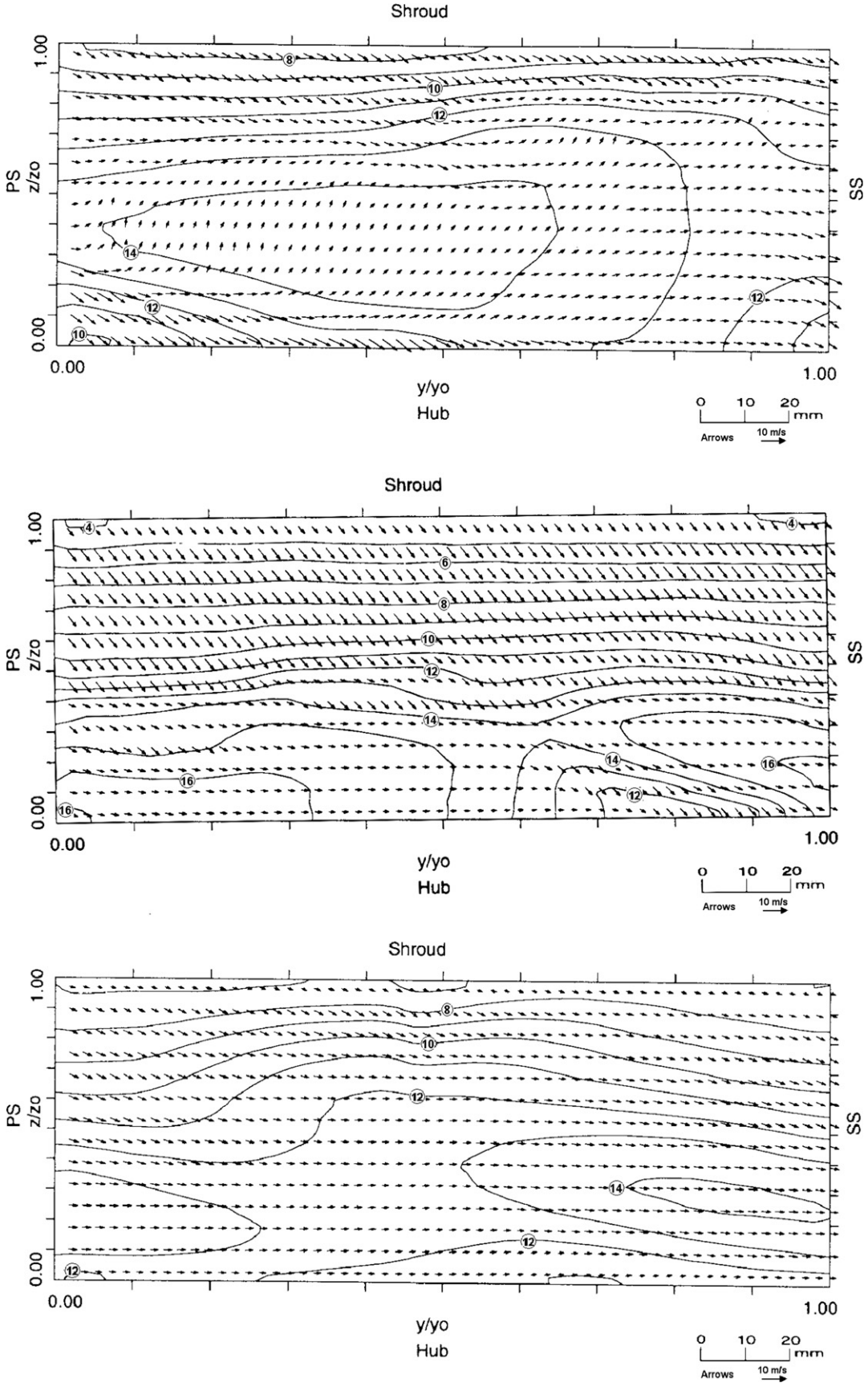

Fig. 9. Mean velocities at station 3 (10%, 50% and 90% vane-to-vane position).

4.2. Station 2

Station 2 is located within the vaneless space close to the vane leading edges. Fig. 6 shows that there are substantial differences between the flow velocities at the three inter-vane positions. The highest velocity region or 'jet' has remained close to the hub at the 10% vane-to-vane position, but thickening of the hub boundary layer at the other two positions has displaced the jet towards the centre of the passage. The highest velocities are still observed at the mid vane-to-vane location, but the differences between the

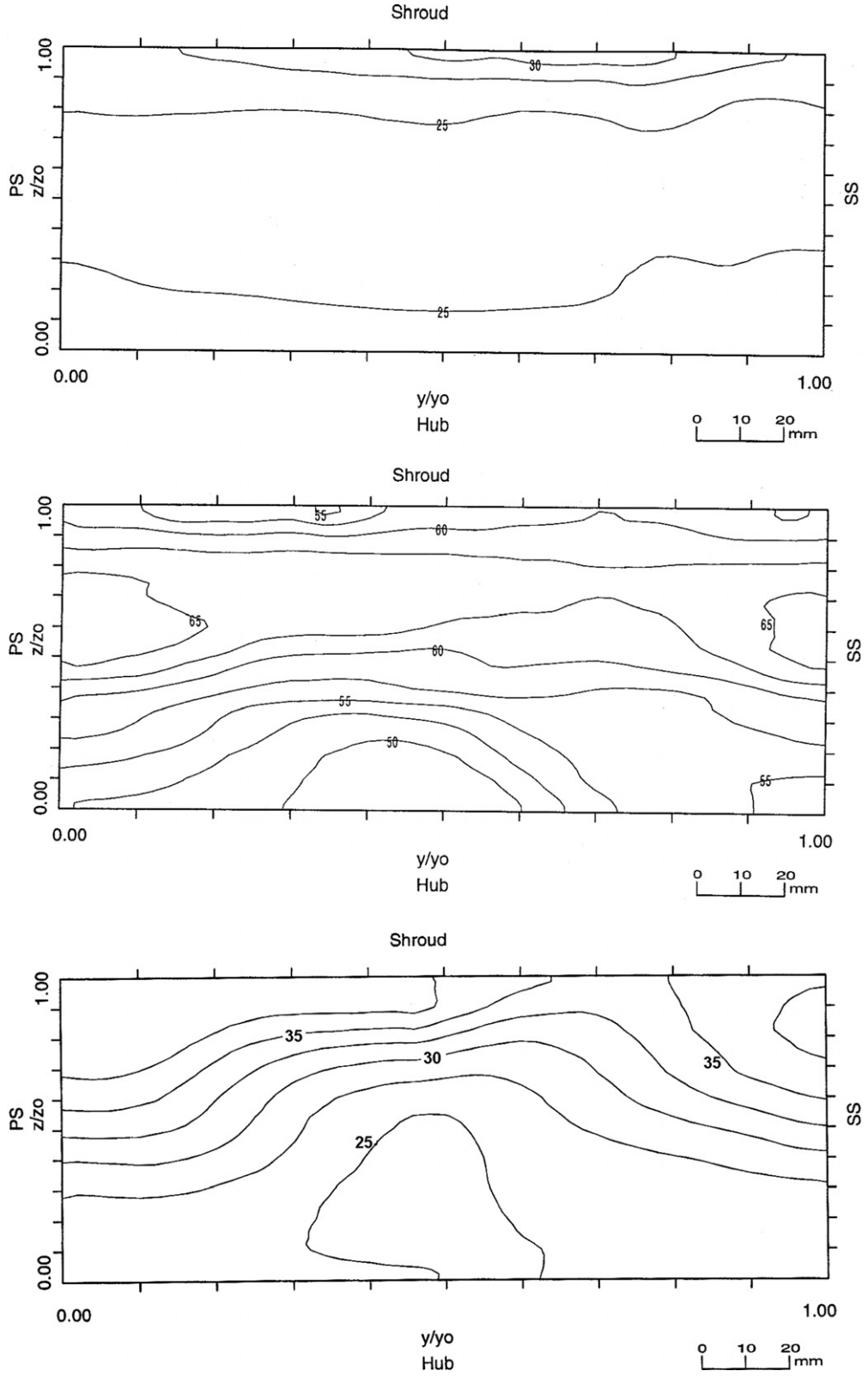

Fig. 10. Flow angle at station 3 (10%, 50% and 90% vane-to-vane position).

three locations is now less marked. The deficit in velocity in the passage wake is little altered from station 1, but the wake has spread across the shroud wall, particularly at the two near vane positions. This is because of the upstream effect of the vanes in moderating the circumferential variations in the tangential/radial flow angle (see Fig. 7), in the near vane positions, the circumferential variation

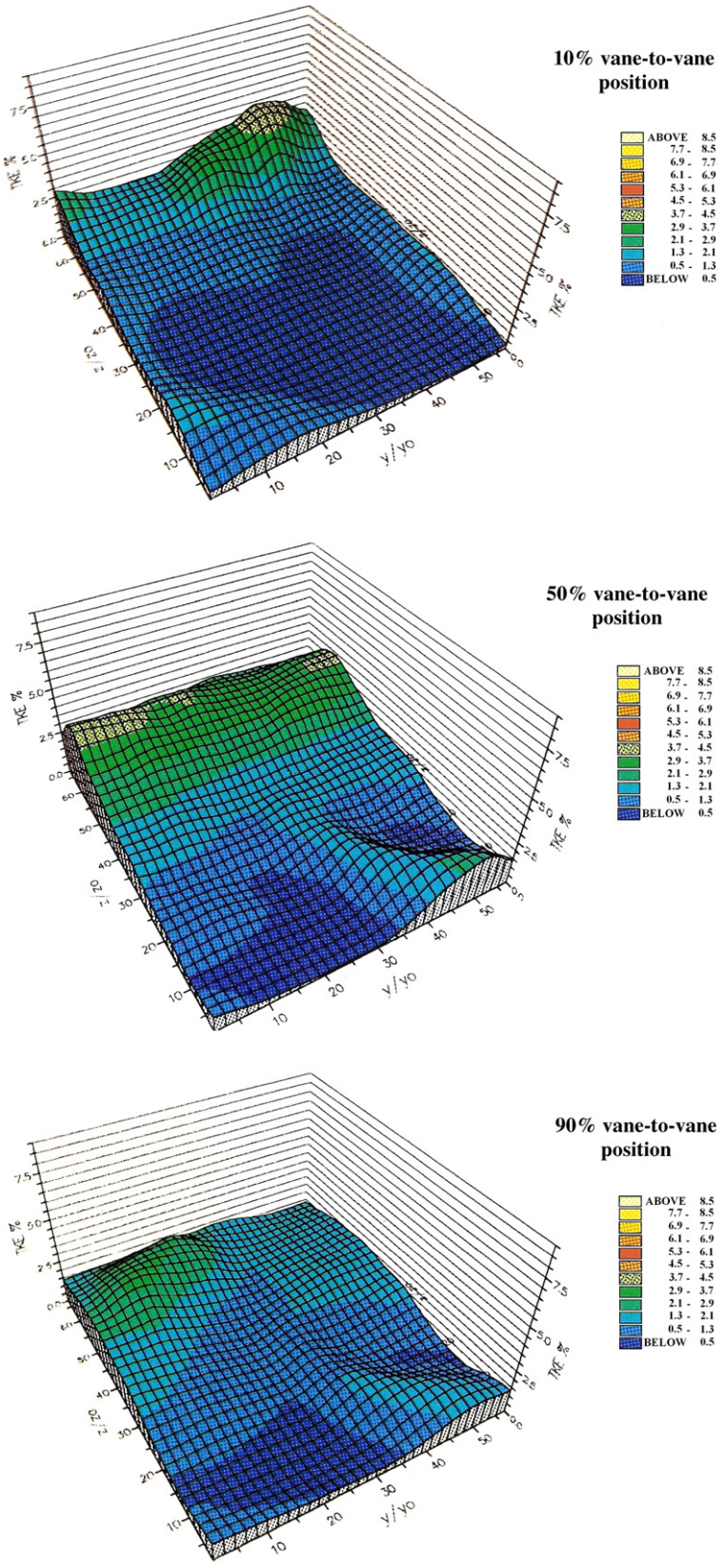

Fig. 11. Turbulent kinetic energy at station 3 (10%, 50% and 90% vane-to-vane position).

in flow angle is less than 10° and so large incidence losses due to flow separation from the vanes can be avoided. There is however significant variation in the flow angle in the axial direction and so some twisting of the blade leading edges would be beneficial. As the circumferential variation in flow angle is greater near the shroud it may also be beneficial to sweep the vane leading edge such that it is located at a lower radius at the hub than at the shroud.

The passage wake has moved across the shroud because of the tangential velocity between stations 1 and 2. The blade wake has also moved in this direction, but by a greater distance near the hub and shroud walls. This is due to the increase in radial/tangential flow angle which is primarily brought about by a decrease in radial velocity. The close proximity of the vanes also has a significant moderating effect on the secondary velocities which are largest at the mid vane position.

The turbulent kinetic energy diagrams (Fig. 8) show how the level within the blade wake has decreased substantially from station 1. The increase in width of the blade wake is also clearly depicted. However, little change is observed in the kinetic energy within the passage wake. These observations are similar to those made for the vaneless diffuser (Pinarbasi and Johnson, 1994), who concluded that the high level of kinetic energy was only associated with high levels of Reynolds stress in the blade wake. The high levels of kinetic energy in the passage wake were attributed to low frequency meandering of the wake position.

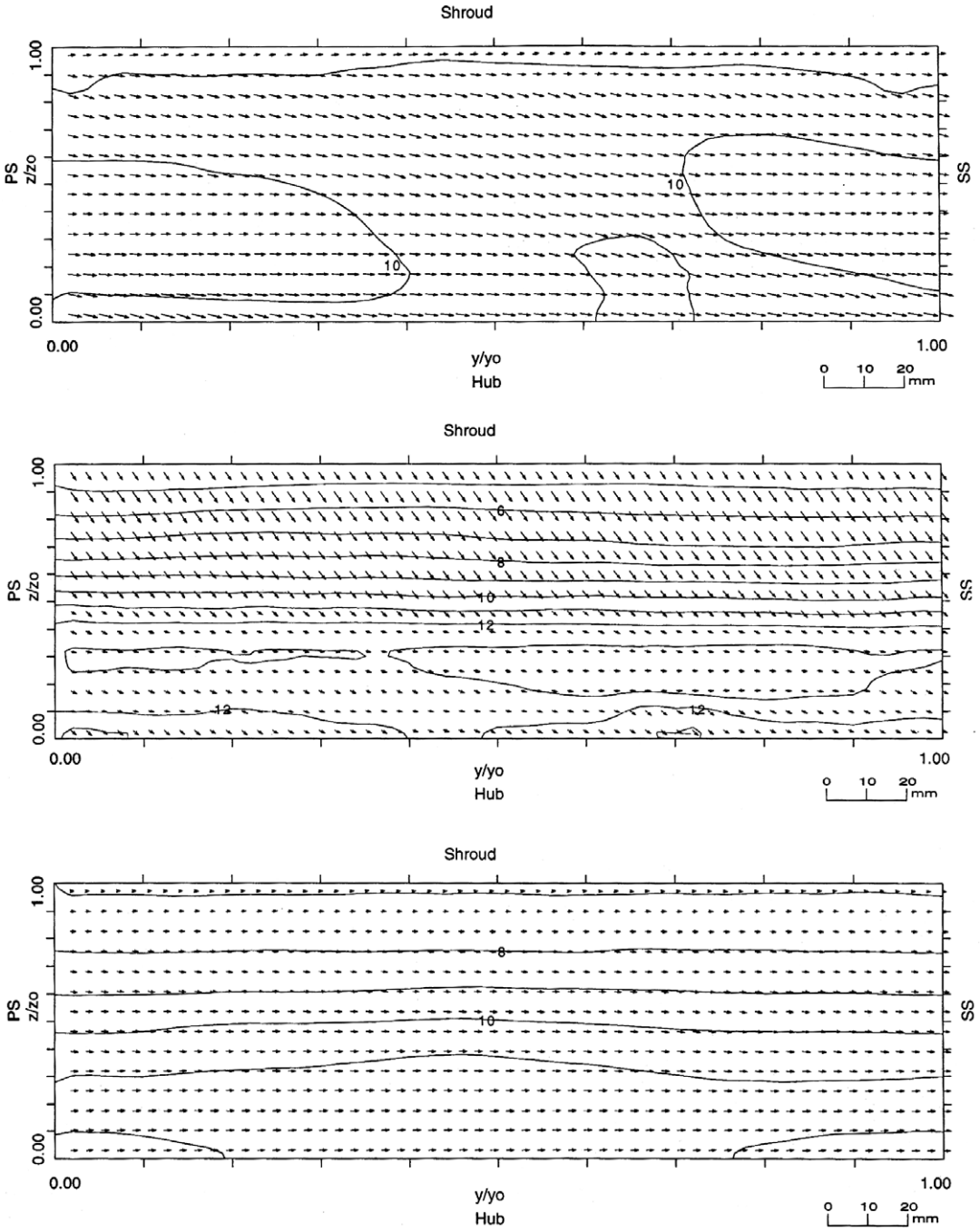

Fig. 12. Mean velocities at station 8 (10%, 50% and 90% vane-to-vane position).

4.3. Station 3

Station 3 is located within the vaned part of the diffuser. The circumferential variations in velocity (Fig. 9) are now generally small. The blade wake has continued to move in the positive y direction most rapidly at the 10% vane-to-vane position and least rapidly at the 90% position. The greatest deficit in velocity is within the blade wake at the mid vane position, where the strongest secondary velocities are also observed. These observations are also supported by the results of Krain (1981) and Inoue (1980).

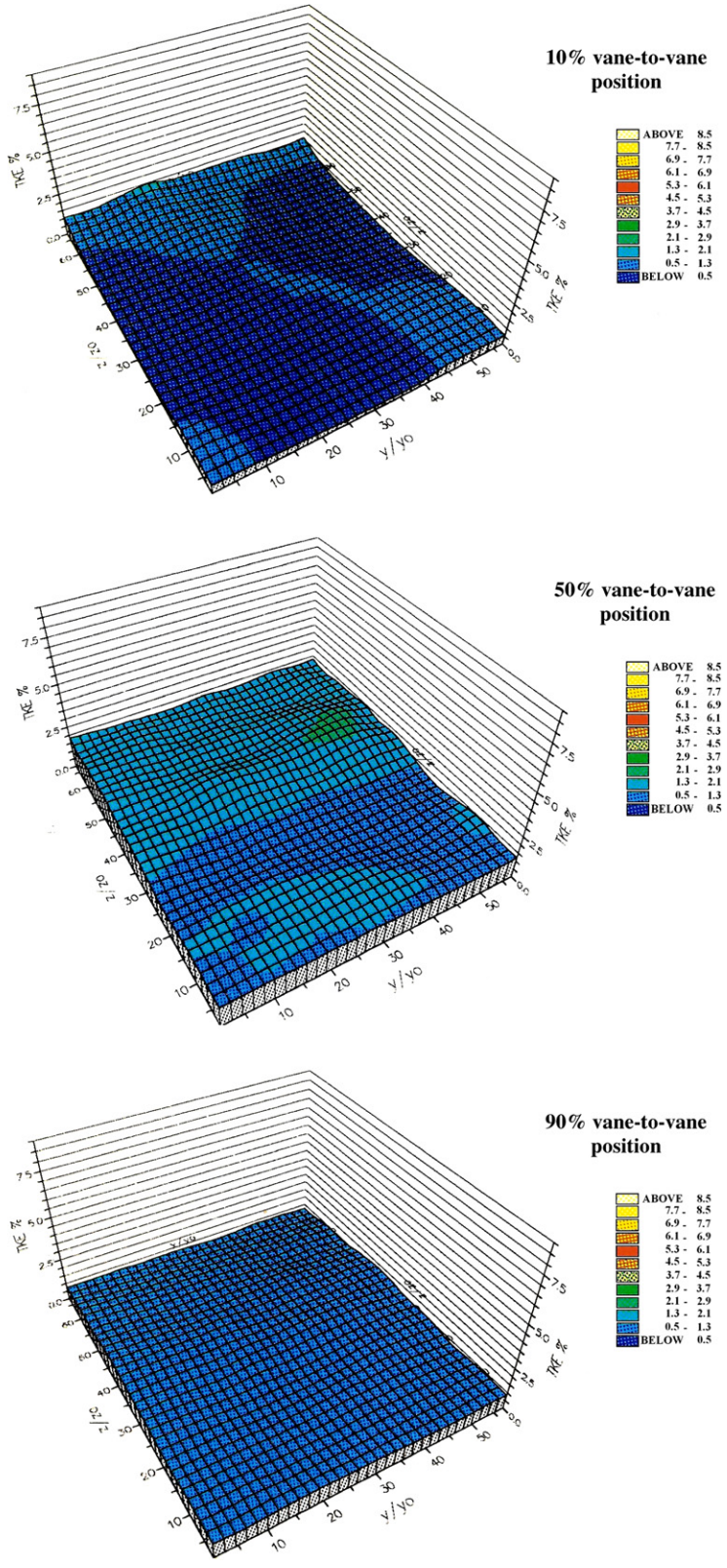

Fig. 13. Turbulent kinetic energy at station 8 (10%, 50% and 90% vane-to-vane position).

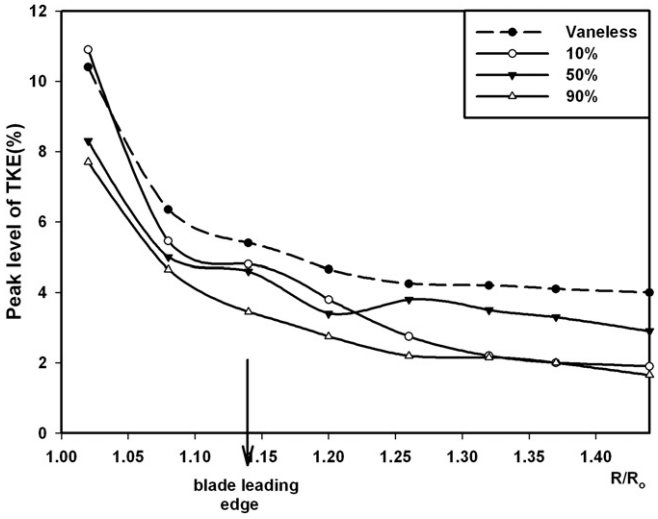

Fig. 14. Blade wake decay in the vaned and vaneless diffusers.

The flow angles (Fig. 10) indicate little circumferential variation and the variations in the axial direction have also moderated from station 2 due to the guiding effect of the vanes. The flow does have a significantly different flow direction at the mid vane position.

The position of the blade wake is highlighted by the kinetic energy diagrams (Fig. 11). The levels within the passage wake have only reduced slightly from station 1.

4.4. Station 8

Changes occur more gradually downstream of station 3 and therefore results are only presented here for station 8. The mean velocities (Fig. 12) show only negligible variations in the circumferential direction. The axial component of velocity is also small except near the shroud at the mid vane position. These cross velocities appear to be associated with the thickening shroud boundary layer which is substantially thicker at the mid vane position than near the vanes.

The turbulent kinetic energy level (Fig. 13) is more or less uniform across the passage with a modest increase in the shroud boundary layer at the mid vane position.

4.5. Blade wake decay

The decay of wakes is commonly quantified using the velocity deficit. For the current results the highly non uniform flow means that the velocity deficit can not be determined accurately. For this reason, the peak turbulent kinetic energy measured within the blade wake, is used here as a measure of the strength of the blade wake as shown in Fig. 14. The blade wake decays more rapidly for the current vaned diffuser than in the vaneless diffuser reported by Pinarbasi and Johnson (1994). The figure also shows quite clearly how the blade leading edge increases the turbulent mixing and how the blade wake mixes out more rapidly close to the vanes than at the mid-vane position.

5. Conclusions

The phase lock loop measurement technique is capable of obtaining accurate detailed measurements in centrifugal compressor diffusers. Measurements show that the flow at the diffuser inlet exhibits similar non-uniformities observed previously at the impeller discharge. It was seen that the presence of vanes in a diffuser significantly influence the flow in the vaneless space. Velocities are increased in the mid vane position and decreased close to the vanes. Mixing out of the blade wakes is seen to be enhanced.

Circumferential variations in velocity are rapidly mixed out in the near vane positions although some variations persist at the mid vane position well into the diffuser.

Large variations in flow angle are observed at the impeller exit, and although this does not appear to lead to separation of the flow from the diffuser vanes, the authors would recommend the twisting of the vane leading edge in the axial direction in order that the risk of flow separation is minimized.

6. Further work

The authors intend to obtain similar test results for further conventional diffuser designs and for a state of the art diffuser designed using an inverse technique (e.g. Zangeneh (1994)). The objective of the work will be to establish to what extent the losses associated with the mixing out of the flow can be reduced using advanced design techniques.

References

Farge, T.Z., Johnson, M.W., 1990. The effect of backswept blading on the flow in a centrifugal compressor impeller. ASME paper 90-GT-231.

Hayami, H. et al., 1990. Application of a low speed solidity cascade diffuser to transonic centrifugal compressor. ASME J. Turbomach. 112, 25–29.

Inoue, M., 1980. Centrifugal compressor diffuser studies. Ph.D. Thesis, University of Cambridge.

Inoue, M., Cumpsty, N.A., 1984. Experimental study of the centrifugal impeller discharge flow in vaneless diffusers. J. Eng. Gas Turb. Power 106, 455–467.

Jorgensen, F.E., 1971. Directional sensitivity of wire and fibre film probes. DISA Inform. 11, 31–37.

Johnson, M.W., Moore, J., 1980. The development of wake flow in a centrifugal compressor. ASME J. Eng. Power 102, 383–390.

Krain, H., 1981. A study on centrifugal impeller and diffuser flow. ASME J. Eng. Power 103, 688–697.

Pinarbasi, A., Johnson, M.W., 1994. Detailed flow measurements in a centrifugal compressor vaneless diffuser. J. Turbomach. 116 (3), 453–461.

Pinarbasi, A., Johnson, M.W., 1995. Off design measurements in a centrifugal compressor vaneless diffuser. J. Turbomach. 117 (4), 602–610.

Pinarbasi, A., Johnson, M.W., 1996. Detailed stress tensor measurements in a centrifugal compressor vaneless diffuser. J. Turbomach. 118 (2), 3 4–399.

Yoshinaga, Y. et al., 1980. Aerodynamic performance of a centrifugal compressor with vaned diffusers. ASME J. Fluids Eng. 102, 486–493.

Zangeneh, M., 1994. Inverse design of centrifugal compressor vaned diffusers in inlet shear flows. ASME paper 94-GT-144.